

The reaction $\gamma p \rightarrow \pi^0 \gamma' p$ and the magnetic dipole moment of the $\Delta^+(1232)$ resonance

M. Kotulla¹, J. Ahrens², J.R.M. Annand³, R. Beck², G. Caselotti², L.S. Fog³, D. Hornidge², S. Janssen¹, B. Krusche⁴, J.C. McGeorge³, I.J.D. McGregor³, K. Mengel¹, J.G. Messchendorp¹, V. Metag¹, R. Novotny¹, M. Pfeiffer¹, M. Rost², S. Sack¹, R. Sanderson³, S. Schadmand¹, D.P. Watts³

¹*II. Physikalisches Institut, Universität Gießen, D-35392 Gießen, Germany*

²*Institut für Kernphysik, Johannes-Gutenberg-Universität Mainz, D-55099 Mainz, Germany*

³*Department of Physics and Astronomy, University of Glasgow, Glasgow G128QQ, UK*

⁴*Department of Physics and Astronomy, University of Basel, CH-4056 Basel (Switzerland)*

(Dated: November 5, 2018)

The reaction $\gamma p \rightarrow \pi^0 \gamma' p$ has been measured with the TAPS calorimeter at the Mainz Microtron accelerator facility MAMI for energies between $\sqrt{s} = 1221\text{--}1331$ MeV. Cross sections differential in angle and energy have been determined for all particles in the final state in three bins of the excitation energy. This reaction channel provides access to the magnetic dipole moment of the $\Delta^+(1232)$ resonance and, for the first time, a value of $\mu_{\Delta^+} = (2.7_{-1.3}^{+1.0}(\text{stat.}) \pm 1.5(\text{syst.}) \pm 3(\text{theo.})) \mu_N$ has been extracted.

PACS numbers: 13.40Em, 14.20.Gk, 25.20.Lj

The complex structure of the nucleon is reflected in its rich excitation spectrum. Attempts to unravel the baryon structure have led to an impressive determination of the properties of the nucleon, e.g. polarizabilities, magnetic moments, and more general form factors. Additional and substantial insight in the parton structure of the nucleon has been gained through deep inelastic electron scattering. In contrast to that, the knowledge of the nucleon's excited states is limited to the mass of the lowest resonances and its (iso)spin quantum numbers. However, to test the modelling of internal degrees of freedom of the excited states, measurements of static properties are required. In particular, the properties of the $\Delta(1232)$ resonance are of considerable interest because of its prominent position in the excitation spectrum.

In this context, the magnetic moment is an important observable for testing theoretical baryon structure calculations. Different predictions for the magnetic moment were made in several calculations [1, 2, 3, 4]. The magnetic moments of the octet of baryons (N, Λ, Σ, Ξ) of the SU(3) flavor symmetry classification are known very accurately through spin precession measurements. However, for the decuplet baryons, only the Ω^- magnetic moment has been determined as the lifetime of the other decuplet members is too short for this technique. If SU(3) flavour symmetry were to hold, the Δ and the nucleon would be degenerate in mass and their magnetic moments related through $\mu_{\Delta} = Q_{\Delta} \mu_p$, where Q_{Δ} is the Δ charge and μ_p the proton magnetic moment. However, structure calculations predict significant deviations from this SU(3) value [1, 2, 3, 4].

It has been proposed that the electromagnetic structure of the Δ can be determined by measuring a γ -transition within the resonance [5]. This method is depicted in Fig. 1, which shows an energy level diagram with the proton (nucleon) as the ground state and the Δ as the first excited state. The Δ structure can be probed by exciting the proton to a Δ , which then emits a real photon and subsequently decays into a nucleon and a

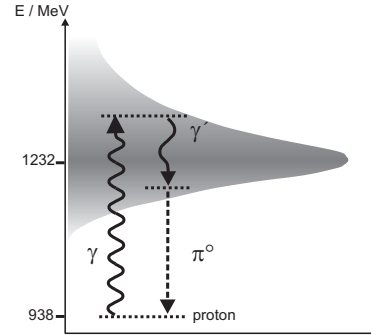


FIG. 1: Method to study the static electromagnetic properties of the $\Delta^+(1232)$ isobar. The γ' transition carries the information of the magnetic moment of the Δ^+ .

pion. Spin and parity conservation require that the lowest order electromagnetic transition is magnetic dipole (M1) radiation. This $\Delta \rightarrow \Delta \gamma'$ amplitude is proportional to μ_{Δ^+} and was recently investigated in theoretical calculations [6, 7, 8]. The next allowed multipole is the electric quadrupole (E2) transition, but this amplitude vanishes in the limit of zero photon energy because of time reversal symmetry [9]. The E2/M1 ratio of the transition amplitude $N \rightarrow \Delta$ has been measured to be very small, approx 0.025 [10], which leads to the assumption that the quadrupole deformation of the Δ is very small. The magnetic octupole (M3) transition is suppressed by two additional powers of photon momentum. Hence, the measurement of the reaction $\gamma p \rightarrow \pi^0 \gamma' p$ provides access to μ_{Δ^+} . Unfortunately this final state can also result from bremsstrahlung radiation of the intermediate Δ and the proton. These contributions are of the same order as the $\Delta \rightarrow \Delta \gamma'$ transition of interest. Nonresonant contributions are expected to play a minor role, since the partial wave decomposition of the related elastic channel $\gamma p \rightarrow \pi^0 p$ shows the dominance of the Δ resonant reaction process [11]. The reaction channel $\gamma p \rightarrow \pi^+ \gamma' n$ is in that sense less favorable for extracting the magnetic

moment of the Δ^+ isobar. An accurate theoretical description of all processes contributing to $\gamma p \rightarrow \pi^0 \gamma' p$ is crucial for extracting a precise value for μ_{Δ^+} .

The magnetic moment of the Δ^{++} isobar was extracted in a similar way from the reaction $\pi^+ p \rightarrow \pi^+ \gamma' p$. Two experiments at the University of California (UCLA) [12] and the Schweizerisches Institut für Nuklearforschung (SIN, now called PSI) [13] have been performed and as a result of many theoretical analyses of these data the Particle Data Group [14] quotes a range of $\mu_{\Delta^{++}} = 3.7\text{--}7.5 \mu_N$ (where μ_N is the nuclear magneton). The large uncertainty in the extraction of $\mu_{\Delta^{++}}$ is due to the strong contribution of π^+ bremsstrahlung and model dependencies. In the reaction channel described here, the bremsstrahlung contributions are much weaker.

The reaction $\gamma p \rightarrow \pi^0 \gamma' p$ was measured at the electron accelerator Mainz Microtron (MAMI) [15, 16] using the Glasgow tagged photon facility [17, 18] and the photon spectrometer TAPS [19, 20]. A quasi-monochromatic photon beam was produced via bremsstrahlung tagging. The photon energy covered the range 205–820 MeV with an average energy resolution of 2 MeV. The TAPS detector consisted of six blocks each with 62 hexagonally shaped BaF₂ crystals arranged in an 8×8 matrix and a forward wall with 138 BaF₂ crystals arranged in a 11×14 rectangle. Each crystal is 250 mm long with an inner diameter of 59 mm. The six blocks were located in a horizontal plane around the target at angles of $\pm 54^\circ$, $\pm 103^\circ$ and $\pm 153^\circ$ with respect to the beam axis. Their distance to the target was 55 cm and the distance of the forward wall was 60 cm. This setup covered $\approx 40\%$ of the full solid angle. All BaF₂ modules were equipped with 5 mm thick plastic detectors for the identification of charged particles. The liquid hydrogen target was 10 cm long with a diameter of 3 cm. Further details are described in [21].

The measurement of the $\gamma p \rightarrow \pi^0 \gamma' p$ reaction channel was exclusive since the 4-momenta of all particles in the final state were determined. The π^0 mesons were detected via their two photon decay channel and identified in a standard invariant mass analysis from the measured photon momenta. The two π^0 decay photons and the γ' photon in the final state were distinguished by using the π^0 invariant mass as a selection criterion. The two photons with an invariant mass closest to the π^0 mass were assigned to be the decay photons. The protons were identified using the excellent time resolution of the TAPS detector and the deposited proton energy: The characteristic time of flight dependence on the energy of the proton and a pulse shape analysis [21] were sufficient to identify the proton uniquely. The proton energy calibration was performed by exploiting energy balance of the exclusively measured $\gamma p \rightarrow \pi^0 p$ channel, thereby compensating for the energy loss in the target and plastic detectors. Random TAPS - tagging spectrometer coincidences were subtracted using background events outside the prompt coincidence time window.

Further kinematic checks were performed by exploiting the kinematic overdetermination of the reaction. Special

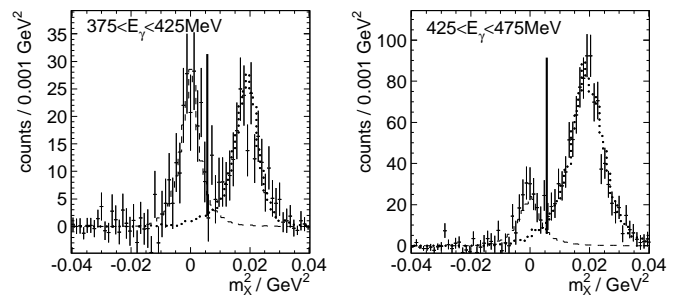


FIG. 2: Missing mass of the $(\pi^0 p)$ system in the final state, but with an additional photon detected for two different incident photon energies. The peak near 0.02 GeV² originates from $2\pi^0$ production and is cut away. The peak at 0 GeV² shows the true $\pi^0 \gamma' p$ production. The dashed and dotted lines show the corresponding simulated lineshapes using GEANT3.

attention had to be paid to background from $2\pi^0$ production arising from events in which one of the four $2\pi^0$ decay photons escaped detection due to the limited solid angle coverage of the detector. In a first step, the conservation of the total momentum was checked in the three cartesian directions respectively. After that, a missing mass analysis was performed to discriminate the $2\pi^0$ contamination. The following missing mass was calculated:

$$M_X^2 = ((E_{\pi^0} + E_p) - (E_{beam} + m_p))^2 - ((\vec{p}_{\pi^0} + \vec{p}_p) - (\vec{p}_{beam}))^2 \quad (1)$$

where E_{π^0} , \vec{p}_{π^0} , E_p , \vec{p}_p denote the energy and momenta of the π^0 and proton in the final state and m_p the proton mass. The resulting distributions (Fig. 2) show two distinct peaks, the widths of which are determined by the detector resolution. The peak near 0.02 GeV² reflects the missing mass of a π^0 and therefore originates from the $2\pi^0$ production, while the peak at 0 GeV² indicates the missing mass of a photon and hence the $\pi^0 \gamma' p$ production. A Monte Carlo simulation of the $2\pi^0$ and $\pi^0 \gamma' p$ reactions using GEANT3 [22] reproduces the lineshape of the measured data. The nearly background free identification of the $\gamma p \rightarrow \pi^0 \gamma' p$ reaction is demonstrated in Fig. 2. The remaining small $2\pi^0$ background due to the finite detector resolution (16% in the highest energy bin) is subtracted for the cross section determination. Since the information of the photon γ' has not been used for evaluating the missing mass defined in Eq. 1, another kinematic check has to prove that the photon γ' is not accidental. Therefore the energy balance was calculated to test energy conservation: $E_{BAL} = (E_{beam} + m_p) - (E_{\pi^0} + E_p + E_{\gamma'})$; the notation is the same as in Eq. 1. The energy balance confirms the clean identification of the $\pi^0 \gamma' p$ reaction channel.

The cross section was deduced from the rate of the $\pi^0 \gamma' p$ events divided by the number of hydrogen atoms per cm², the photon beam flux, the branching ratio of π^0 decay into two photons, and the detector and analysis efficiency. The intensity of the photon beam was determined by counting the scattered electrons in the tagger

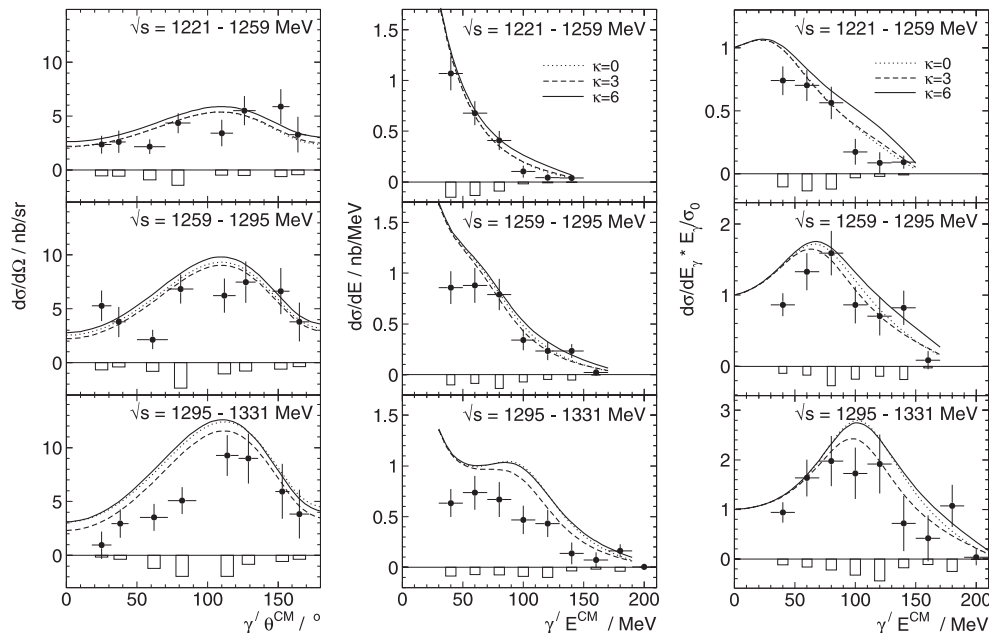


FIG. 3: Differential cross sections for three different incident excitation energies \sqrt{s} in the CM frame. The systematic errors are shown as a bar chart. *Left*: angular distribution of the photon γ' ; *middle*: energy distribution. The lines show the calculation [9] for three different values of the anomalous magnetic moment $\kappa_{\Delta^+} = 0, 3$ and 6 . On the *right* side, the energy distribution has been divided by the prediction of the soft photon limit $\frac{\sigma_0}{E_{\gamma'}}$, respectively for the data and the calculation.

focal plane and measuring the loss of photon intensity with a 100%-efficient BGO detector which was moved into the photon beam at lowered intensity. The geometrical detector acceptance and analysis efficiency due to cuts and thresholds were obtained using the GEANT3 code and an event generator producing distributions of the final state particles according to [9]. The systematic errors of the efficiency determination are small because the shape of the measured distribution is reproduced by the simulation. The average value for the detection efficiency is 0.25%.

The measured differential cross sections for the reaction $\gamma p \rightarrow \pi^0 \gamma' p$ are shown in Fig. 3 for three different incident excitation energies \sqrt{s} (i.e. the total γp center of mass energy), starting at the Δ resonance position and going up to 100 MeV above it. The angular distribution of the photon γ' in the CM system shows an enhancement for angles around 120° . The energy distribution shifts towards higher γ' energies with rising \sqrt{s} , showing an $1/E_{\gamma'}$ form with an additional peak, where the strength and the position depend on the excitation energy \sqrt{s} . The different reaction mechanisms suggest such a behavior, where the $1/E_{\gamma'}$ dependence stems from the external bremsstrahlung of the proton in the final state. The position of the peak structure (the energy of γ') originating partly from the Δ radiation is determined by the difference of \sqrt{s} and the Δ peak mass and a small correction due to the available phase space. The Δ decay mechanism contribution is emphasized, when the energy differential cross section is divided by $1/E_{\gamma'}$ (compare the column on the right hand side of Fig. 3).

The first series of calculations, including only the resonant $\Delta \rightarrow \Delta \gamma'$ process as indicated in Fig. 1, were done by Machavariani et al. [6, 7] and Drechsel et al. [8]. Both groups use the effective Lagrangian formalism and in addition the latter group uses a quark model approach to describe the reaction. Since these calculations consider only the Feynman diagram which is sensitive to μ_{Δ^+} , they cannot reproduce the measured cross sections.

Recently, Drechsel and Vanderhaeghen [9] extended their model and included bremsstrahlung diagrams (resonant Δ , non-resonant Born diagrams and ω exchange). This calculation is shown in comparison to the measured cross sections in Fig. 3. The overall shape is reproduced very well, although the absolute value is overestimated for the highest excitation energy. This is related to an overestimate in the calculation of the reaction $\gamma p \rightarrow \pi^0 p$, which is well understood and attributed to πN rescattering contributions [9]. A model independent determination of the $\pi^0 \gamma' p$ cross section is feasible in the soft photon limit, which relates $\pi^0 \gamma' p$ production to $\pi^0 p$ production in the limit of vanishing photon energy $E_{\gamma'}$ [23]:

$$\lim_{E_{\gamma'} \rightarrow 0} \left(\frac{d\sigma}{dE_{\gamma'}} \right) = \frac{1}{E_{\gamma'}} \cdot \sigma_0 \quad (2)$$

$$\sigma_0 = \int d\Omega_{\pi^0} \left(\frac{d\sigma}{d\Omega_{\pi^0}} \right) \cdot \frac{2\alpha_{em}}{\pi} \left\{ \left(\frac{v^2+1}{2v} \right) \ln \left(\frac{v+1}{v-1} \right) \right\}$$

$$v = \sqrt{1 - \frac{4m_p^2}{t}} \quad , \quad t = (k - p_{\pi^0})^2$$

$d\sigma/d\Omega_{\pi^0}$ labels the differential cross section for $\pi^0 p$ production, m_p the proton mass, t the four momentum transfer between the initial photon and the π^0 meson and $\alpha_{em} = e^2/4\pi \approx 1/137$. According to Eqn. 2, the energy differential cross section divided by $\sigma_0/E_{\gamma'}$ should be equal to 1 in the limit of zero photon energy $E_{\gamma'}$. This ratio is shown in the right column of Fig. 3, where the differential cross section $d\sigma/d\Omega_{\pi^0}$ in Eqn. 2 is calculated with the same effective Lagrangian model [9]. For comparison to the experimental results, the data are also plotted as a cross section ratio where σ_0 has been determined from Eqn. 2 using consistently the measured differential cross section $d\sigma/d\Omega_{\pi^0}$ of the $\gamma p \rightarrow \pi^0 p$ reaction. The cross section ratios show better agreement; they are less sensitive to uncertainties in the model calculation as well as uncertainties in the determination of the photon flux and target length.

The sensitivity to the magnetic moment of the Δ^+ is illustrated in Fig. 3 by the difference of the three curves. The Δ^+ magnetic moment can be obtained from the anomalous magnetic moment κ_{Δ^+} which is the only free parameter of the calculation [9]

$$\mu_{\Delta^+} = (1 + \kappa_{\Delta^+}) \cdot \frac{e}{2m_{\Delta}} = (1 + \kappa_{\Delta^+}) \cdot \frac{m_N}{m_{\Delta}} \cdot \mu_N \quad (3)$$

where $\mu_N = e/2m_N$ is the nuclear magneton. A combined maximum likelihood analysis [14] of the three cross section ratios in Fig. 3 yields a value of $\mu_{\Delta^+} = (2.7^{+1.0}_{-1.3} \pm 1.5)\mu_N$, the goodness of fit is $\chi^2/F = 1.8$ ($F=21$). The first error represents the statistical uncertainty and the second one reflects the systematic errors given in Fig. 3. This error does not include the systematic error of the model calculation which is of the order of $\pm 3\mu_N$, estimated from the uncertainties discussed in [9]. The extracted value of μ_{Δ^+} is in the range of dif-

ferent baryon structure calculations [1, 2, 3, 4], but not sensitive enough to discriminate between them.

In conclusion, we have made the first measurement of the magnetic moment of the $\Delta^+(1232)$ resonance by exploiting the reaction $\gamma p \rightarrow \pi^0 \gamma' p$. We see a clear deviation from a soft bremsstrahlung cross section at higher energies of the radiated photon, pointing to a sensitivity to the magnetic moment of the $\Delta^+(1232)$ resonance. However, the limited statistics and the uncertainty of the model lead to a value of the $\Delta^+(1232)$ magnetic moment, which is not sufficiently precise for a detailed test of different baryon structure calculations. This situation calls for a follow up experiment with much higher statistical precision, using so that the kinematic regions most sensitive to μ_{Δ^+} can be exploited [9, 24]. An investigation of the cross section asymmetry using a polarized photon beam would also be valuable. Supplementary, an improvement in the theoretical description is necessary to minimize the model dependence. The measurement can be extended to higher excited states of the nucleon. In particular the magnetic moment of the $S_{11}(1535)$ resonance is accessible via the reaction $\gamma p \rightarrow \eta \gamma' p$ because of its clean distinction from other resonances in the second resonance region through the η channel.

It is a pleasure to acknowledge inspiring discussions with M. Vanderhaeghen, D. Drechsel, A. Machavariani and A. Faessler. We would like to thank the accelerator group of MAMI as well as many other scientists and technicians of the Institut fuer Kernphysik at the University of Mainz for the outstanding support. This work is supported by DFG Schwerpunktprogramm: "Untersuchung der hadronischen Struktur von Nucleonen und Kernen mit elektromagnetischen Sonden", SFB221, SFB443, the UK Engineering and Physical Sciences Research Council and Schweizerischer Nationalfond.

-
- [1] D. Leinweber, T. Draper, and R. Woloshyn, Phys. Rev. D **46**, 3067 (1992).
[2] M. Butler, M. Savage, and R. Springer, Phys. Rev. D **49**, 3459 (1994).
[3] H. Kim, M. Praszalowicz, and K. Goeke, Phys. Rev. D **57**, 2859 (1998).
[4] T. Aliev, A. Özpineci, and M. Savci, Nucl. Phys. A **678**, 443 (2000).
[5] L. Konratyuk and L. Ponomarev, Yad. Fiz. 7 (1968) 11 [Sov. J. Nucl. Phys. 7 (1968) 82] **82** (1968).
[6] A. Machavariani, A. Faessler, and A. Buchmann, Nucl. Phys. A **646**, 231 (1999).
[7] A. Machavariani, A. Faessler, and A. Buchmann, Nucl. Phys. A **686**, 601 (2002).
[8] D. Drechsel, M. Vanderhaeghen, et al., Phys. Lett. B **484**, 236 (2000).
[9] D. Drechsel and M. Vanderhaeghen, Phys. Rev. C **64**, 065202 (2001).
[10] R. Beck et al., Phys. Rev. Lett. **78**, 606 (1997).
[11] D. Drechsel, O. Hanstein, S. Kamalov, and L. Tiator, <http://www.kph.uni-mainz.de/MAID> (2000).
[12] B. Nefkens et al., Phys. Rev. D **18**, 3911 (1978).
[13] A. Bosshard et al., Phys. Rev. D **44**, 930 (1991).
[14] D. Groom et al., Eur. Phys. J. **C15**, 1 (2000).
[15] T. Walcher, Prog. Part. Nucl. Phys. **24**, 189 (1990).
[16] J. Ahrens, H. Backe, D. von Harrach, H. Kaiser, F. Klein, R. Neuhausen, and T. Walcher, Nuclear Physics News **4**, 5 (1994).
[17] I. Anthony, J. Kellie, S. Hall, G. Miller, and J. Ahrens, Nucl. Instr. Meth. **A 301**, 230 (1991).
[18] S. Hall et al., Nucl. Instr. Meth. **A 368**, 698 (1996).
[19] R. Novotny, IEEE Trans. Nucl. Sci. **38**, 379 (1991).
[20] A. R. Gabler, Nucl. Instr. Meth. **A 346**, 168 (1994).
[21] R. Novotny et al., IEEE Trans. Nucl. Sci. **43**, 1260 (1996).
[22] R. Brun et al., *GEANT3 Users Guide*, CERN, Data Handling Division DD/EE/84-1 (1986).
[23] M. Vanderhaeghen and D. Drechsel, *private communication* (2002).
[24] M. Kotulla, Acta Phys. Polon. B **33**, 957 (2002).